
This is an electronic reprint of the original article.
This reprint may differ from the original in pagination and typographic detail.

Leppänen, Elli; Peltonen, Antti; Seitsonen, Jani; Koskinen, Jari; Laurila, Tomi

Effect of thickness and additional elements on the filtering properties of a thin Nafion layer

Published in:
Journal of Electroanalytical Chemistry

DOI:
[10.1016/j.jelechem.2019.05.002](https://doi.org/10.1016/j.jelechem.2019.05.002)

Published: 15/06/2019

Document Version
Peer-reviewed accepted author manuscript, also known as Final accepted manuscript or Post-print

Published under the following license:
CC BY-NC-ND

Please cite the original version:
Leppänen, E., Peltonen, A., Seitsonen, J., Koskinen, J., & Laurila, T. (2019). Effect of thickness and additional elements on the filtering properties of a thin Nafion layer. *Journal of Electroanalytical Chemistry*, 843, 12-21. <https://doi.org/10.1016/j.jelechem.2019.05.002>

This material is protected by copyright and other intellectual property rights, and duplication or sale of all or part of any of the repository collections is not permitted, except that material may be duplicated by you for your research use or educational purposes in electronic or print form. You must obtain permission for any other use. Electronic or print copies may not be offered, whether for sale or otherwise to anyone who is not an authorised user.

Effect of thickness and additional elements on the filtering properties of a thin Nafion layer

Elli Leppänen^a, Antti Peltonen^b, Jani Seitsonen^c, Jari Koskinen^d, Tomi Laurila^{a*}

^a Department of Electrical Engineering and Automation, School of Electrical Engineering, Aalto University, PO Box 13500, 00076 Aalto, Finland

^b Aalto-NanoFab, Micronova, Aalto University, PO Box 13500, 0076 Aalto, Finland

^c Nanomicroscopy Center, Department of Applied Physics, School of Science, Aalto University, PO Box 15100, 00076 Aalto, Finland

^d Department of Materials Science and Engineering, School of Chemical Technology, Aalto University, PO Box 16200, 00076 Aalto, Finland

* Corresponding author: tomi.laurila@aalto.fi

Abstract

Nafion is widely used as a filtering membrane in electroanalytical applications to improve selectivity towards cations. However, the role of the thickness of Nafion on its electroanalytical performance is poorly understood. Furthermore, Nafion is often modified with additional elements without characterizing their influence on Nafion's filtering properties. To understand in-depth these uncharacterized effects on Nafion, we approach these issues systematically by studying first (*i*) the role of Nafion film thickness on top of a well characterized tetrahedral amorphous carbon electrode and second (*ii*) introducing nanodiamonds into the same Nafion films with different thicknesses. With careful electrochemical and structural analyses, we show that already ultrathin Nafion film significantly reduces limiting currents of anionic species $\text{IrCl}_6^{3-/4-}$ and uric acid. With a thicker film ($\sim 3.6 \mu\text{m}$) the selective nature of Nafion is demonstrated as anionic species are completely filtered and enrichment of cationic species $\text{Ru}(\text{NH}_3)_6^{2+/3+}$ is achieved. However, diffusion within the film controls the overall kinetics of the cation reactions and the electrochemical performance of Nafion is heavily dependent on the width of the potential window used. In addition, we show that modifying Nafion with nanodiamonds increases permeability of both cationic and anionic species. Hence, Nafion's ability for selective detection of cations is greatly reduced. Interestingly, chemical effects were also observed between nanodiamonds and an inner sphere redox probe uric acid. Thus, additional elements in Nafion do not only affect the physical structure of the film, but may produce chemical changes as well. Based on the results presented here, we emphasize the importance of an in-depth investigation to understand the case specific effects of modified Nafion films to guarantee the reliability of the sensor devices in the final application.

Keywords Nafion; nanodiamonds; tetrahedral amorphous carbon; rotating disk electrode; selectivity

1. Introduction

Nafion, a sulfonated copolymer, is an extensively used material in electroanalytical applications for detecting biomolecules. Its hydrophilic SO_3^- groups form negatively charged channels inside the polymer [1]. Due to the electrostatic forces, Nafion enables the enrichment of positively charged cations and rejects negatively charged anions. Since the common interferents in physiological environments are anionic ascorbic acid (AA) and uric acid (UA), Nafion is widely used for the selective detection of different biomolecules due to its ability to reduce the signals of these species. In particular, numerous studies have been done with selective detection of dopamine [2,3] and glucose [4,5]. Furthermore, Nafion is a popular material in chemical- and biosensors for its antifouling properties [6].

Despite the attractive properties of Nafion, the effect of Nafion layer thickness on its performance is still not unambiguously established. This is the case especially with the very thin films used in neutral (physiological) solutions. The influence of Nafion film thickness has been mainly characterized for hydrogen fuel cell applications, where acidic media are used [7,8]. In studies where electrochemical sensors have been developed for the detection of different biomolecules, Nafion thickness has rarely been experimentally characterized nor optimized [3,5,9]. As the membrane thickness has a significant effect on the performance of an electroanalytical device such as response time, permeability and ability to resist interferents, characterization of the thickness dependence of these properties is required in order to understand the analytical performance of Nafion.

In addition to inadequate characterization of the Nafion film itself, it is very common that other materials such as carbon nanotubes [9,10], metallic nanoparticles [11,12] or other polymers [12,13] are incorporated into Nafion to enhance the electrodes sensitivity towards the target analyte. As Nafion is further modified with these materials, complexity of the structure increases making it even harder to understand the relationship between material properties and the electroanalytical performance. Usually characterization of the structural changes induced by the introduced material and how these modifications affect Nafion's ability to detect cations selectively are either insufficient or totally lacking. Hence it is poorly understood how Nafion's electroanalytical performance in selective detection of biomolecules is altered by modifying it with other materials.

Here, we combine Nafion with a tetrahedral amorphous carbon (ta-C) thin film in which the structure and electrochemical properties has been characterized in great detail in recent years [14–18]. ta-C has several characteristics that makes it attractive material for electrochemical sensors such as low background current, wide potential window, chemical inertness [19] and excellent antifouling

properties [20]. Moreover, we have shown that ta-C is suitable material for detection of DA [21], morphine [22], tramadol and O-desmethyltramadol [23]. As Nafion is combined together with this well characterized material, it is possible to study the role of the polymer film thickness on the electrochemical performance.

To investigate how the modification of Nafion with other materials alters its electroanalytical performance, we have introduced detonation nanodiamonds (DND) with a diameter of 4 to 6 nm into the Nafion film. DNDs are produced by detonation of solid explosives [24]. Around nanodiamonds crystalline sp^3 core exists a thin sp^2 shell functionalized with oxygen and nitrogen containing groups [25–27]. Even though sp^3 is an insulating material the sp^2 -rich surface layer is conductive and DNDs have in fact shown high electrochemical activity towards several redox probes such as ruthenium [28], iridium chloride [29], ferrocenemethanol [30] and ferrocyanide [28,31,32]. This electrochemical activity has been suggested to arise due to the high content of oxygen containing surface groups [27,28,33]. In addition to this character, low concentrations of DNDs are also biocompatible [34] making DNDs attractive material for electrochemical sensing of biomolecules. In fact, we have previously shown that DNDs on top of ta-C enhances sensitivity towards dopamine [34].

Hence, in this work, we study the influence (i) of Nafion film thickness and (ii) addition of nanodiamonds on its electroanalytical performance in the detection of cationic and anionic species. Investigation is carried out by utilizing a careful combination of structural and electrochemical characterization methods.

2. Experimental

2.1. Sample fabrication

ta-C films were deposited on p-type (100) conductive Si wafers with 0.001-0.002 Ω cm resistivity (Ultrasil, USA). First, a 20 nm Ti interlayer was deposited on Si wafer by direct current magnetron sputtering. After this step, 7 nm ta-C film was deposited on top of the Ti using a pulsed filtered cathodic vacuum arc (p-FCVA). More detailed description of the deposition process can be found from Palomäki et al. (2017). After fabrication the wafer was diced into 0.7 x 0.7 cm pieces with an automated dicing saw.

Three types of Nafion electrodes were prepared by drop casting 7 μ l of 0.1 wt-%, 9 μ l of 1 wt-% and 5 wt-% Nafion solution on top of ta-C. The Nafion solutions with concentrations of 0.1 wt-% and 1 wt-% were prepared by diluting 5 wt-% Nafion 117 (Aldrich) with 99.5% EtOH (Altia, Finland) in ratios 1:50 and 1:5.

Nanodiamond + Nafion composite films were fabricated using same Nafion concentrations as above. First carboxyl functionalized nanodiamond-water suspension (Carbodeon, Finland) with concentration of 5 wt-% was diluted with ethanol to 0.05 wt-% and sonicated for 20 minutes. Next three DND+Nafion composite solutions were prepared by diluting 0.05 wt-% DND solution to 0.005 wt-% either with 0.1 wt-%, 1 wt-% and 5 wt-% Nafion. Composite solutions were sonicated for 20 minutes and afterwards DND +Nafion electrodes were fabricated by drop casting 7 μ l of 0.1 wt-%, 9 μ l of 1 wt-% and 5 wt-% composite solution on top of ta-C.

2.2. Characterization of Nafion thickness

Thickness of the Nafion films were characterized with scanning electron microscope (SEM). Before imaging, cross-sectional samples were prepared with focused ion beam (FIB) milling. Both procedures were carried out with FEI Helios NanoLab 600 dual-beam system.

Before the ion milling, 0.1 wt-%, 1 wt-% and 5 wt-% Nafion electrodes were fabricated with 100 nm of aluminium and 2 μ m of platinum. In order to avoid melting of Nafion under ion and e-beams, low voltages and currents were used. Preparation of cross-sections was carried out with 15 kV acceleration voltage in rough milling and 280/460 pA currents. SEM study of the cross-sections was conducted with 5-15 kV and low currents of 86-43 pA. The working distance during the operations was 4.1 mm.

2.3. TEM

Nanodiamonds distribution in 0.1% and 5% Nafion films were characterized with cryo-TEM. Investigated samples were fabricated by drop-casting composite solution prepared as above on top of Si substrate with area of 25 mm². DND + 5% Nafion solution was drop-casted with volume of 3 μ l, whereas DND + 0.1% Nafion sample was prepared by drop-casting 20 x 7 μ l of solution to obtain thicker film for characterization. After drying the composite films in fume hood for 10 minutes, both samples were submerged into deionized water. Wet DND + Nafion films were detached from the Si substrate with tweezers and floated on top of copper TEM grid with non-continuous holey carbon film (Agar Scientific). Micrographs containing only Nafion and DNDs are obtained by imaging composite film at the regions of holes in holey carbon film.

Samples were imaged perpendicular to the composite film surface using JEOL JEM-3200FSC transmission electron microscope operated at 300kV under zero-loss conditions. The samples were maintained at liquid nitrogen temperature during imaging. Acquired TEM images were processed with Digital Micrograph software (Gatan).

2.4. Electrochemical measurements

Electrochemical investigation of Nafion thin film coatings were carried out with both conventional cyclic voltammetry (CV) and using a rotating disk electrode (RDE) configuration. Experiments were conducted with a Gamry Reference 600+ potentiostat. A three-electrode cell was used with an Ag/AgCl reference electrode (Radiometer Analytical) and a Pt wire (Goodfellow) counter electrode.

The effect of (i) film thickness and (ii) addition of nanodiamonds on Nafion's electrochemical performance were both investigated using RDE configuration with rotational frequencies of $\omega = 400, 900, 1600$ & 2500 rpm. RDE experiments were conducted in $1 \text{ mM Ru(NH}_3)_6^{2+/3+}$, $1 \text{ mM IrCl}_6^{3-/4-}$ and $1 \text{ mM uric acid (UA)}$ solutions, where hexaamineruthenium(III) chloride (Sigma-Aldrich) and potassium hexachloroiridate(IV) (Aldrich) were dissolved in 1 M KCl (Merck Suprapur, pH 6.8), whereas uric acid (Sigma) in $10 \text{ mM phosphate buffered saline (PBS, pH 7.4)}$. New electrodes ($r = 2.5 \text{ mm}$) were used for every electrochemical experiment. All electrodes with Nafion film were immersed into the solution 10 min prior to the measurement for proper hydration.

The solutions were purged with N_2 for at least 30 min before the experiments. All the measurements were carried out at room temperature in a Faraday's cage.

3. Theory

RDE is a powerful method for characterizing the effect of Nafion film on the overall reaction rate as it enhances the mass transport into the electrode through convection. Hence, a steady state can be achieved.

For electrochemically reversible reactions, the mass transport (diffusion) limiting current i_d follows the Levich equation [35]

$$i_d = \pm 0.62nFAD^{2/3}\nu^{-1/6}c^b\omega^{1/2} \quad (1)$$

where n is number of electrons in the reaction, F the Faraday constant, A area of the electrode D the diffusion coefficient of the reactant, ν the kinematic viscosity of the electrolyte, c^b the bulk concentration of the reactant and ω the rotation rate of the electrode. From equation (1) it is observed that i_d is function of rotation rate and linearly dependent on $\omega^{1/2}$. Hence, the mass transport rate increases with a faster rotation speed. The overall current i measured under quasi/irreversible conditions at the bare electrode is related to the diffusional current and true kinetic current i_k , which represents current in the absence of any mass-transfer effects. i given by [35]

$$1/i = 1/i_d + 1/i_k \quad (2)$$

where

$$i_k = nFAk_h c^b \quad (3)$$

Here k_h is rate constant for heterogeneous reaction at the electrode. Kinetic current i_k can be evaluated from linear Koutecký -Levich plot ($1/i$ vs. $1/\omega^{1/2}$) by extrapolating experimental data to $\omega^{-1/2} = 0$. As $\omega \rightarrow \infty$, the intercept yields $1/i_k$.

With Nafion/ta-C electrodes, additional mass-transport resistance is produced by the Nafion film. Therefore, diffusion within the film must be taken into account. Here we will assume that the kinetic current i_k is same for each electrode (ta-C) and difference in the intercept in Koutecký -Levich plot is caused by the Nafion film. Rate constant k_h' for Nafion/ta-C electrodes is now given by

$$k_h' = k_h + m_T \quad (4)$$

where m_T is the mass transfer coefficient describing the mass transfer effects through the Nafion film.

Gough and Leyplot [36,37] have proposed an alternative model for diffusion in Nafion film, where intercept in Koutecký -Levich plot is sum of $1/i_k$ and diffusional current $1/i_f$. However, we did not consider this model especially practical for our case as evaluation of mass-transport within their approach requires knowledge of the analyte concentration within the film, which is not easy to obtain. Here equations (2) – (4) enables estimation of m_T at mixed region with bulk concentration.

4. Results and Discussion

4.1. SEM – Nafion film thickness

The cross-sectional SEM images for 1% and 5% Nafion/ta-C are presented in Figure 1, where estimated thicknesses are 180 ± 20 nm and 3.6 ± 0.2 μ m, respectively. For 0.1% Nafion/ta-C polymer film could not be observed within the resolution limits of SEM (Fig. S1 in supplementary information). However, when the electrochemical performance of bare ta-C and 0.1% Nafion/ta-C is compared, significant differences can be seen (discussed further in 4.3). Therefore, we propose that 0.1% Nafion forms a very thin (tens of nanometers thick, possibly partly non-continuous) film on top of ta-C.

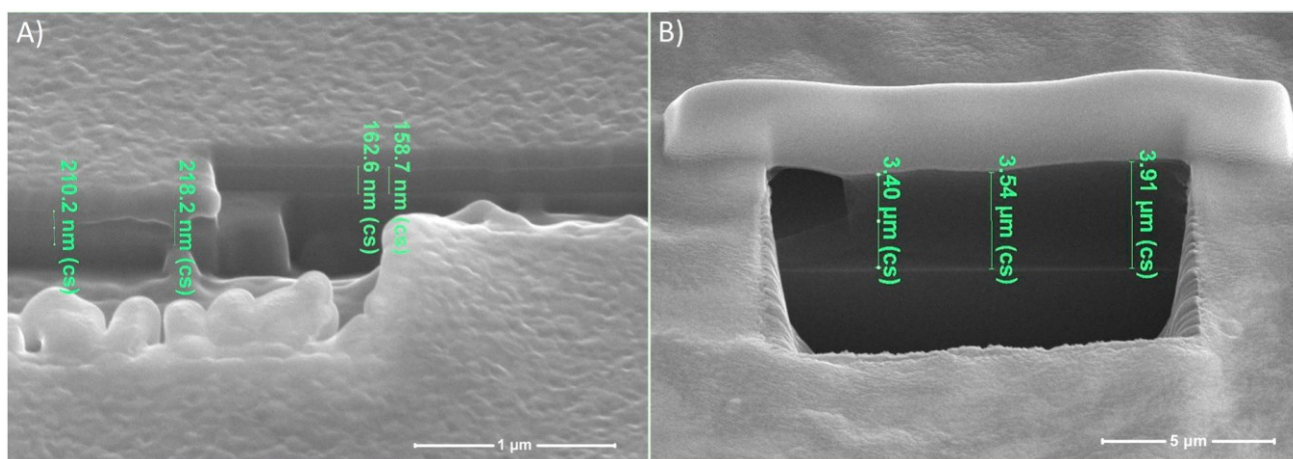


Figure 1 Cross-sectional SEM images of A) 1% Nafion/ta-C and B) 5% Nafion/ta-C electrodes, where thicknesses of the films were evaluated with SEM/FIB system software.

4.2. TEM – DNDs distribution in Nafion

Distributions of nanodiamonds in 0.1% and 5% Nafion film are presented in Figures 2A and 2B. As seen from the HRTEM images, DNDs are agglomerated as also observed elsewhere [38]. Based on qualitative image analysis of the HRTEM-micrographs, in more diluted Nafion (0.1 %) ND agglomerate size is approximately a few tens of nanometers (Fig. 2C). For 5% Nafion size of the aggregates is slightly larger. It should be noticed that DND + 0.1% Nafion TEM sample (Fig. 2A) contains 20 layers of composite solution in order to obtain thicker film for the sample preparation. Therefore, concentration of DNDs is higher than in samples used in electrochemical experiments. Moreover, the thickness of Nafion film varies in HRTEM image due to the multilayer composite as seen from the contrast changes in Figure 2A. However, these results provide background information to address the question of how aggregate size alters Nafion with different thicknesses. In case of 0.1% Nafion, DND aggregates are most likely not incorporated inside the very thin film, but instead exist as agglomerates on top or partly penetrating the film. Conversely, with $\sim 3.6 \mu\text{m}$ thick film (5% Nafion) it is likely that the small aggregates (with respect to film thickness) of DNDs are mixed into the Nafion film itself. Depending on if the DND aggregates are introduced into thin or thick Nafion film, electrochemical response changes significantly (discussed further in 4.4).

High-magnification image of nanodiamond agglomerate is presented in Figure 2D from where crystalline planes for diamond can be observed. FFT of this image shows cubic diamond phase from where measured d-spacing is 1.97 \AA . This correspond closely to value 2.06 \AA for plane $\{111\}$ found from literature for cubic diamond nanoparticles [39,40].

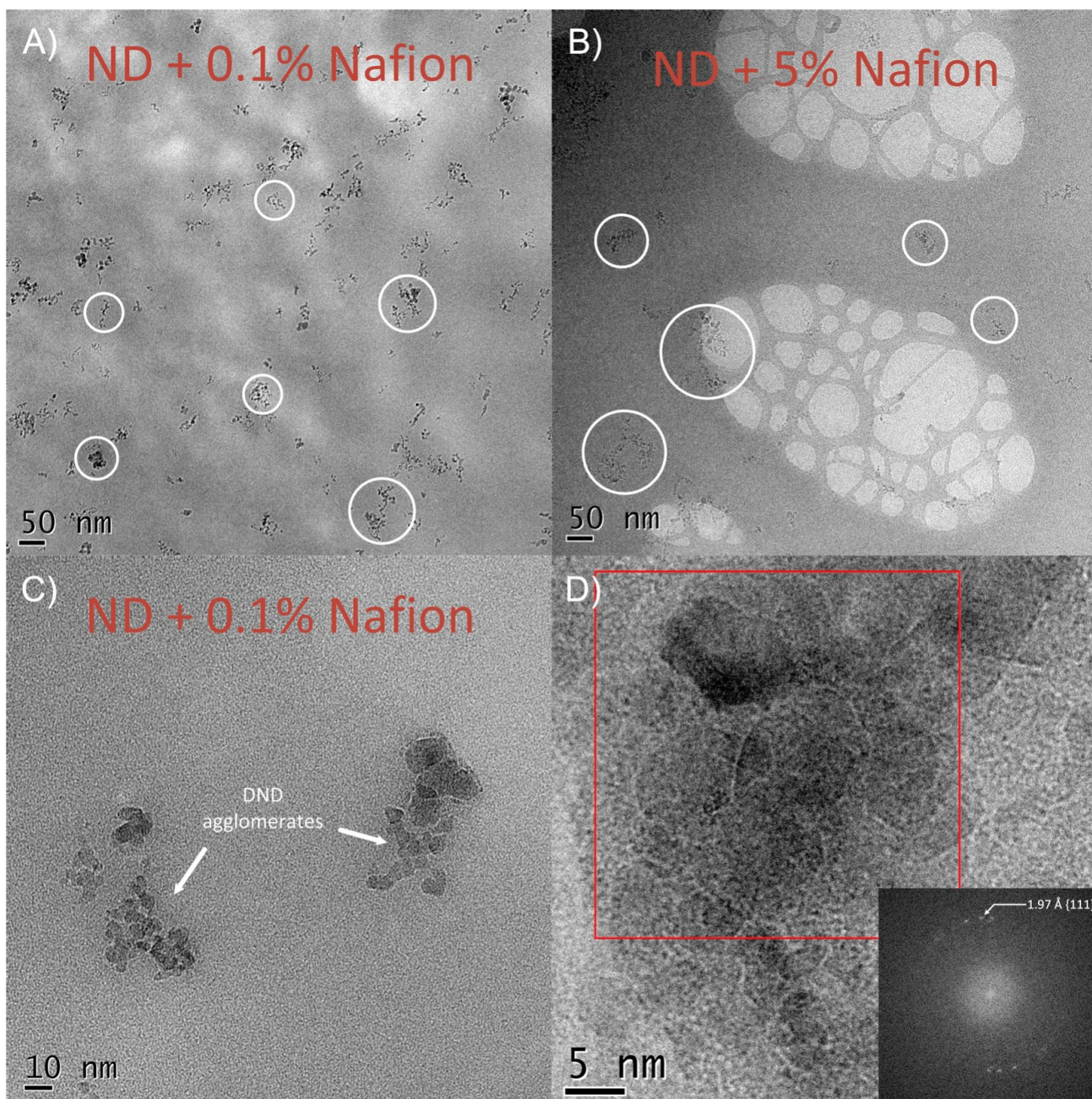


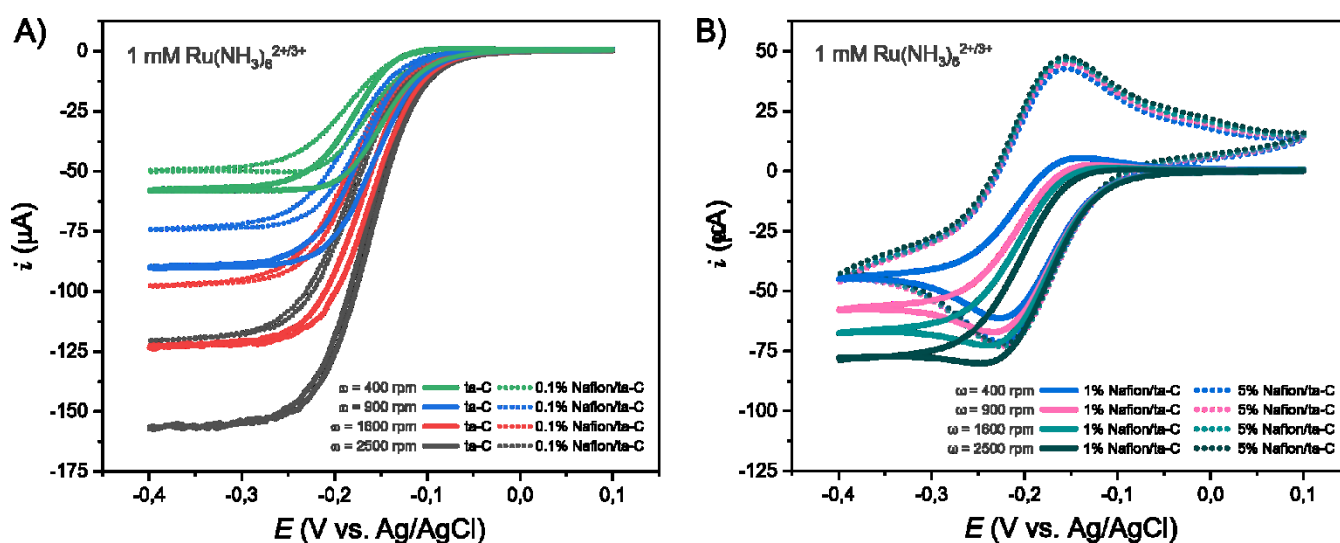
Figure 2 Cryo-TEM micrographs from the DND + Nafion films. Nanodiamond distribution in A) 0.1% Nafion and B) 5% Nafion film, where DND aggregates are marked with white circles. Globular network observed in B) is the holey carbon film. C) High magnification micrographs from DND agglomerates in 0.1% Nafion. D) HRTEM image of DND agglomerate in Nafion, where FTT is taken from area indicated with red square. Intensity of FTT pattern is low due to the low concentration of DNDs. (For interpretation of the references to colour in this figure legend, the reader is referred to the web version of this article.)

4.3. Effect of Nafion film thickness on detection of cations and anions

Nafion interactions with cationic and anionic species was studied using outer sphere redox probes $\text{Ru}(\text{NH}_3)_6^{2+/3+}$ and $\text{IrCl}_6^{3-/4-}$. As these redox systems are surrounded by a strong hydration shell they do not show marked adsorption and are therefore insensitive to the surface chemistry. Thus, the interaction between Nafion and outer sphere probe can be considered to be mainly electrostatic. In addition, negatively charged inner sphere uric acid was used to characterize Nafion ability to reduce

access of anionic species with surface specific interaction to the ta-C surface. UA was chosen for these experiments as it is a common interfering species in physiological environments. The influence of Nafion film thickness on $\text{Ru}(\text{NH}_3)_6^{2+/3+}$, $\text{IrCl}_6^{3-/4-}$ and UA redox reactions was investigated with cyclic voltammetry together with rotating disk electrode configuration.

Hydrodynamic voltammograms for bare ta-C and 0.1% Nafion/ta-C in $\text{Ru}(\text{NH}_3)_6^{2+/3+}$ are shown in Figure 3A. Interestingly, 0.1% Nafion already clearly reduces limiting current when compared to bare ta-C electrode. These findings indicate that 0.1% Nafion solution produces very thin (perhaps somewhat uneven) film on top of ta-C as suggested above. More significant decrease in limiting current is observed with 1% Nafion/ta-C (Fig. 3B). As seen from Figure 3B, diffusion of $\text{Ru}(\text{NH}_3)_6^{2+/3+}$ within the 1% film dominates the overall kinetics as RDE response starts to look more like a conventional CV and the effect of rotating speed diminishes. This is seen to be true especially with lower rotation speeds, where almost CV-like behavior is seen. As the rotation speed is increased, the mass transport limited current is achieved. However, the currents in all cases are significantly smaller than those of ta-C or ta-C + 0.1% Nafion.



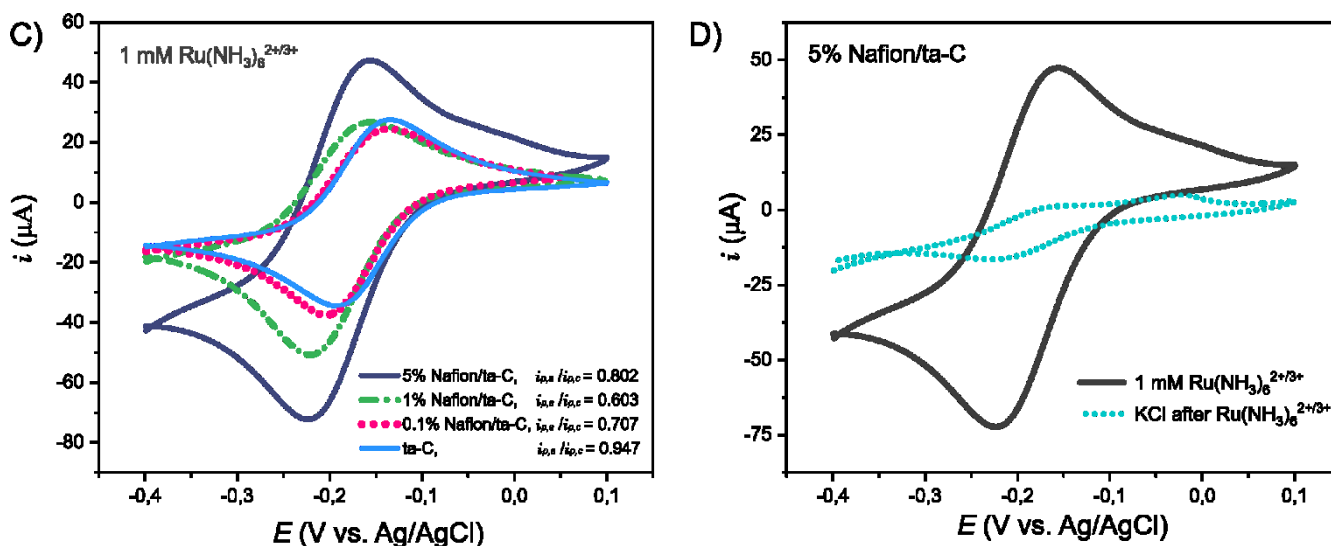
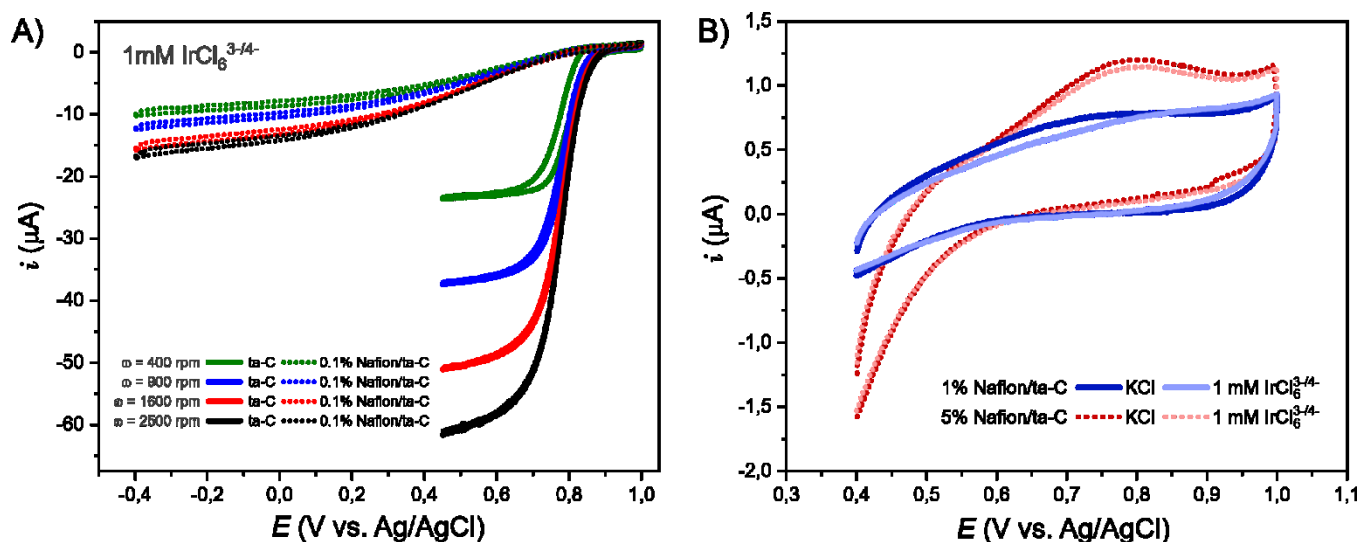


Figure 3 Nafion/ta-C electrodes electrochemical behavior in 1 mM $\text{Ru}(\text{NH}_3)_6^{2+/3+}$ in 1 M KCl. Hydrodynamic voltammograms of A) bare ta-C, 0.1% Nafion/ta-C, B) 1% Nafion/ta-C and 5% Nafion/ta-C. C) Response and peak current ratio $i_{p,a}/i_{p,c}$ for all electrodes. D) 5% Nafion/ta-C in 1 M KCl ($t = 10$ min) after cycling in 1 mM $\text{Ru}(\text{NH}_3)_6^{2+/3+}$. For all measurements $v = 50$ mV/s.

In the case of 5% Nafion/ta-C (Fig. 3B) rotation speed does not seem to have any effect on the overall kinetics as with every ω the response is the same i.e. steady state is not achieved with 5% Nafion. The aqueous volume accessible to ions of either charge is a small fraction of the overall volume of Nafion, and therefore it is expected that the mass transfer of the cations is also affected by the film. In addition, as the film grows in thickness the percolation can become more difficult as all the channels are not interconnected or do not necessarily continue through the whole film. Thus, it is evident that Nafion establishes a diffusion barrier at the interface that reduces the overall kinetics of these cationic species. It is proposed that in the case of 5% Nafion diffusion through ~ 3.6 μm thick film completely controls the overall reaction. As seen from Figures 3A and 3B, it is clear that diffusion within the film becomes more dominating as Nafion film thickness increases. This finding is further supported by the estimated values of mass-transport coefficients m_T in Nafion film (Table S1).

The interaction between Nafion and $\text{Ru}(\text{NH}_3)_6^{2+/3+}$ was studied by measuring CVs for every electrode in cationic $\text{Ru}(\text{NH}_3)_6^{2+/3+}$. With increasing Nafion thickness (Fig. 3C), it is observed that (i) the peak currents are enhanced and (ii) Nafion does not significantly alter the electron transfer kinetics as for 5% Nafion/ta-C $\Delta E_p = 67$ mV and for bare ta-C $\Delta E_p = 58$ mV, respectively. Therefore, it is concluded that at least some ruthenium enriches into the film. This assumption is further supported by the results with high scan rates of 5 and 10 V/s (Fig. S2), where ΔE_p values are approximately the same as in Figure 3C. These results indicate that some of the ruthenium is trapped in the film. Interaction between $\text{Ru}(\text{NH}_3)_6^{2+/3+}$ and Nafion is suggested to be mainly physisorption as properties of 5% Nafion/ta-C are recovered after insertion to pure KCl (Fig. 3D).

Interestingly, the peak current ratio $i_{p,a}/i_{p,c}$ in Figure 3C decreases with Nafion/ta-C electrodes when compared to the bare ta-C. Wopschall and Shain [41] have shown that cathodic current enhances when the oxidation product is weakly adsorbed on the electrode surface. In case of ta-C/Nafion electrodes, it is probable that the oxidation product Ru^{3+} (with higher oxidation state) is electrostatically trapped inside of the Nafion film. Thus, more Ru^{3+} is available for the reduction reaction. Alternatively, Nafion may also act as a barrier that prevents Ru^{3+} for escaping from the electrode surface to the bulk solution. RDE results with anionic $\text{IrCl}_6^{3-/4-}$ and UA are presented in Figure 4. With both analytes limiting current is significantly reduced with 0.1% Nafion/ta-C (Fig. 4A and 4C). These results clearly indicate that already with very thin Nafion film the access of anions on the electrodes surface is strongly suppressed. In case of $\text{IrCl}_6^{3-/4-}$ (Fig. 4A) 0.1% Nafion thin film reduces limiting current approximately to one tenth when compared to bare ta-C electrode. Furthermore, 0.1% Nafion/ta-C shows sluggish kinetics at the mixed region. Similar behavior is observed with UA (Fig. 4C). In addition, it should be noticed that 0.1% Nafion is not enough to completely block $\text{IrCl}_6^{3-/4-}$ and UA.



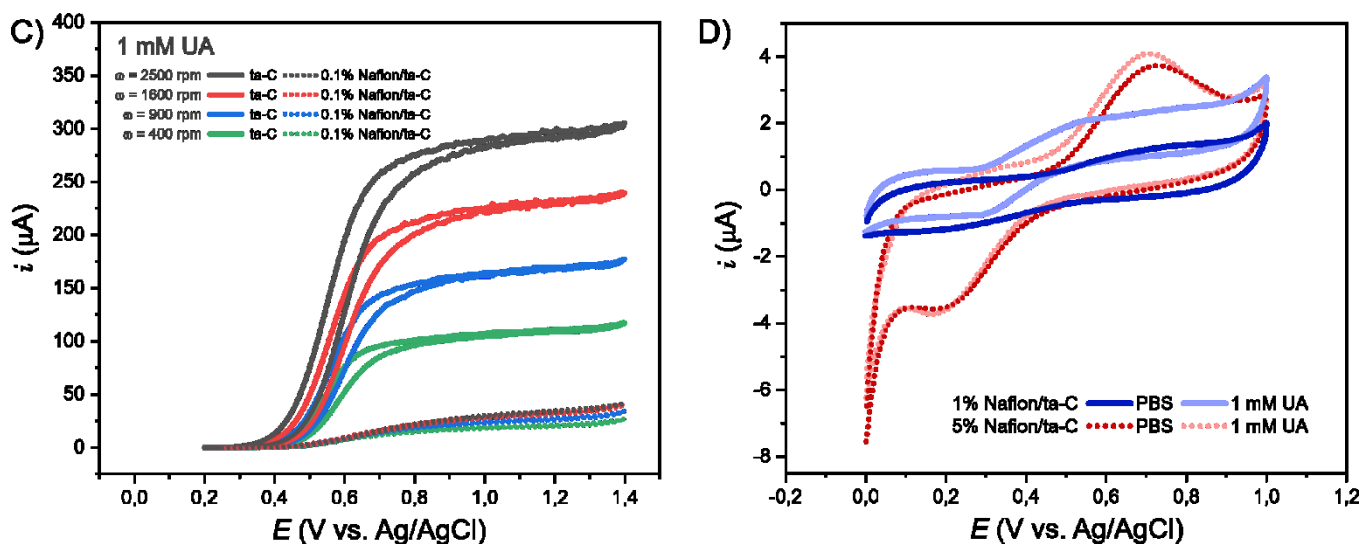


Figure 4 Nafion electrochemical performance in solution containing anionic species. Hydrodynamic voltammograms for bare ta-C and 0.1% Nafion/ta-C in A) 1 mM $\text{IrCl}_6^{3-/4-}$ in KCl and C) 1 mM UA in PBS. Cyclic voltammograms are presented for 1% and 5% Nafion/ta-C in B) 1 mM $\text{IrCl}_6^{3-/4-}$ and D) 1 mM UA as rotation did not have any influence on the response. Scan rate for all measurements $v = 50$ mV/s.

In case of 1% and 5% Nafion/ta-C rotation did not have any effect on the performance of the electrode in $\text{IrCl}_6^{3-/4-}$ and UA solutions. Thus, only conventional cyclic voltammograms are shown for the thicker films in Figure 4B and 4D. From these results it is observed that the addition of $\text{IrCl}_6^{3-/4-}$ or UA into supporting electrolyte does not remarkably change the response of the electrode i.e. CV with or without the anodic species give a rise to similar response. This strongly indicates that the thicker Nafion films block the access of anionic species to the electrode surface very effectively.

Interestingly, as backgrounds in KCl or PBS are measured for the thickest Nafion film some faradaic processes and/or adsorption of ions takes place on/in the film. Figures 3D, 4B and 4D demonstrated that reaction(s) in 5% Nafion film are dependent on the potential window. When measuring $\text{Ru}(\text{NH}_3)_6^{2+/3+}$, reaction(s) most likely originating from Nafion are not seen within the narrow potential window used (-0.4 V to 0.1 V) whereas clear peaks at ~ 0.2 V and ~ 0.75 V are observed when wider potential window is utilized.

As rotation does not have any effect on the performance of 1% and 5% Nafion/ta-C electrodes and addition of $\text{IrCl}_6^{3-/4-}$ and UA does not change the response of the measured signal, it is suggested that thicker Nafion films (i) effectively block anionic species and (ii) reaction(s) observed in 5% Nafion arises from the film itself. Alternatively, if $\text{IrCl}_6^{3-/4-}$ or UA permeates through the film, the oxidation of these species on ta-C surface may be masked by Nafion own characteristic reactions. Oxidation of IrCl_6^{4-} and UA takes place at ~ 0.8 V and ~ 0.7 V (Fig. S3 A and S3 B), respectively, which are at the same position as Nafion own oxidation peak.

To summarize, results clearly show that an already a very thin Nafion film significantly reduces signals arising from anionic species. In addition, strong enrichment of ruthenium is seen with thicker Nafion films. This may be exploited by allowing pre-concentration of cationic analytes of interest to build up before the analysis. However, results in uric acid and iridium chloride demonstrate importance of optimizing Nafion film thickness. The thinnest film does not completely block the signal of the anionic compounds, whereas the thicker (5%) Nafion films generate their own faradic processes and mass-transfer effects that can mask the reaction of the investigated species.

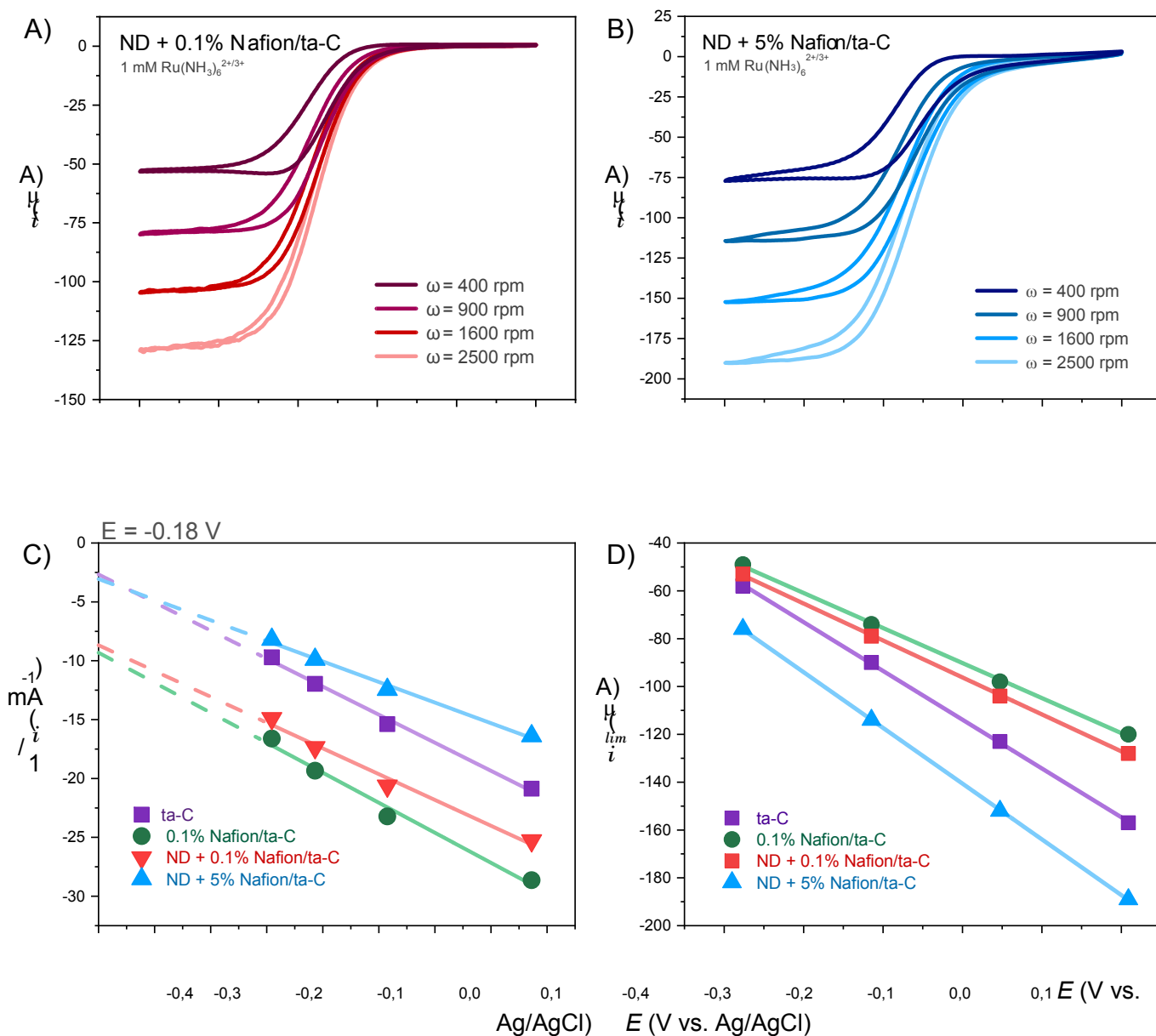
4.4. Effect of modifying Nafion films with nanodiamonds

Nafion is rarely used as a pure material for selective detection of cations. In most cases the properties of Nafion based sensors are further modified by combining Nafion with other materials to enhance catalytic properties. For example graphene [3], carbon nanotubes [10,42] or metallic nanoparticles [11,43] are used to enhance sensitivity towards dopamine. Furthermore, selectivity of the sensors are often increased by adding enzymes into the Nafion matrix to detect for example glucose [9,12] and glutamate [44,45]. However, these studies typically lack characterization of how the modification of Nafion with other structures alters its filtering performance against interfering anionic compounds. As composite materials give rise to complicated interactions, it is extremely difficult to evaluate the relationship between material properties and electrochemical behaviour. Thus, an in-depth investigation is required to understand the case specific effects of modification of Nafion with other materials.

To study the effect of modifying Nafion with other structures, we introduced nanodiamonds into identical Nafion/ta-C electrodes investigated in section 4.3. The utilization of similar Nafion thin films as in previous section, enables comparison of the DND + Nafion composite results to those from plain Nafion films discussed above. Experiments were conducted in an identical manner explained in 4.3 with $\text{Ru}(\text{NH}_3)_6^{2+/3+}$, IrCl_6^{4-} and UA. Here results for DND + 0.1% and DND + 5% Nafion/ta-C are shown as these composite films represents most extreme cases of how DNDs affect Nafion's electroanalytical performance. Results for DND + 1% Nafion/ta-C can be found from the supplementary information.

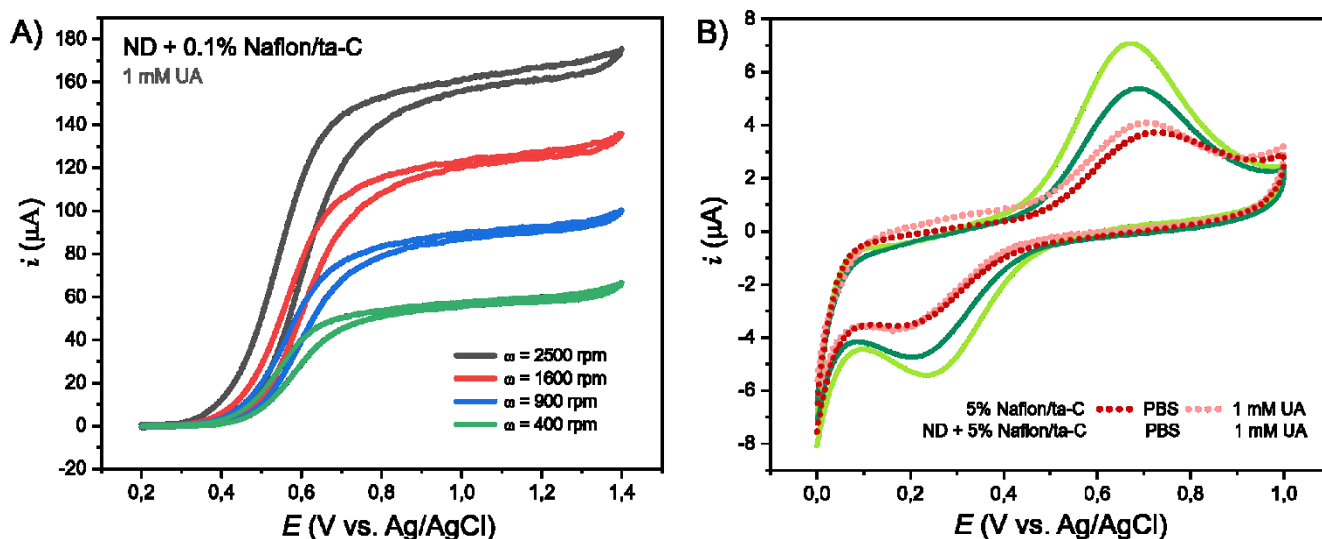
Hydrodynamic voltammograms for DND + 0.1% and DND + 5% Nafion/ta-C in $\text{Ru}(\text{NH}_3)_6^{2+/3+}$ are shown in Figure 5A and 5B. Comparison of these results to plain ta-C and Nafion/ta-C electrodes are illustrated in Figures 5C and 5D by utilizing both Koutecký -Levich and Levich plots. From the Koutecký – Levich plot the kinetic current for plain ta-C is clearly smaller than that of 0.1% Nafion/ta-C confirming the earlier suggestion that a very thin film of Nafion already influences the overall

reaction rate of the electrode. As DNDs are mixed with 0.1% Nafion, no significant difference is observed in the performance of the very thin Nafion film as i_k and i_{lim} are similar to those of 0.1% Nafion/ta-C. Similar behavior was observed between 1% Nafion and DND + 1% Nafion film (Fig. S4). Interestingly, performance of DND + 5% Nafion/ta-C electrode differ completely from plain 5% Nafion/ta-C. As DNDs are incorporated in thicker Nafion film, steady-state is achieved with RDE and diffusion within the composite film does not anymore control the overall reaction. $\text{Ru}(\text{NH}_3)_6^{2+/3+}$ most likely leaks through the film and electron transfer at ta-C surface controls the overall reaction as i_k for DND + 5% Nafion/ta-C is similar to ta-C kinetic current. Estimated values for m_T (Table S1) also demonstrate similar behavior in composite films. Mass-transport effects through DND + 5% Nafion film is reduced compared to DND + 0.1% Nafion indicating that a thicker composite film does not act as a diffusion barrier anymore.



increase substantially. Electrostatic forces arising from negatively charged SO^{3-} channels are inadequate to block $\text{IrCl}_6^{3-/4-}$ in the presence of DNDs. Interestingly this is not seen with the thinnest Nafion films. Based on TEM micrographs in section 4.2, the approximate size of aggregates exceeds the thickness of the very thin 0.1% Nafion film. Therefore, it is assumed that DND aggregates only cause stochastic discontinuities in the 0.1% Nafion film as the properties of the film are not changed. However, in the case of 5% Nafion the DND aggregates are well mixed inside the polymer film. This is suggested to give rise to more complex interactions between DNDs and Nafion as seen from Figures 5B and 6B. However, based on the results above it is difficult to evaluate if the increase in permeability of the films is due to the changes in the physical and/or chemical structure of Nafion. Chemical changes in the structure may arise from the interactions between Nafion and DNDs carboxyl groups with negative zeta potential [34]. However, this effect must be further investigated using DNDs with different surface functionalities in DND + Nafion composites.

Selectivity of the DND + Nafion composite film was studied by measuring anionic inner sphere redox couple uric acid, which is sensitive to surface chemistry. Surprisingly, already with DND + 0.1 % Nafion/ta-C a significant difference is observed in comparison with plain 0.1% Nafion/ta-C. As DNDs are introduced in 0.1% Nafion film, limiting currents increase remarkably (see Fig. 4C and 7A). Drastic effect of introducing DNDs to 0.1% Nafion film is not observed with outer-sphere probes $\text{Ru}(\text{NH}_3)_6^{2+/3+}$ and $\text{IrCl}_6^{3-/4-}$, where interactions are considered to be mainly electrostatic. In the case of plain ta-C, measured i_{lim} values compared to composite film are somewhat smaller. However, as seen from Koutecký–Levich plot (Fig. 7C) DND + 0.1% Nafion/ta-C kinetics at the mixed region is similar to ta-C. Hence, both of these electrodes can detect UA whereas plain 0.1% Nafion film reduces significantly the signal of UA. Based on this result, thin DND + 0.1% Nafion film lacks selectivity towards UA.



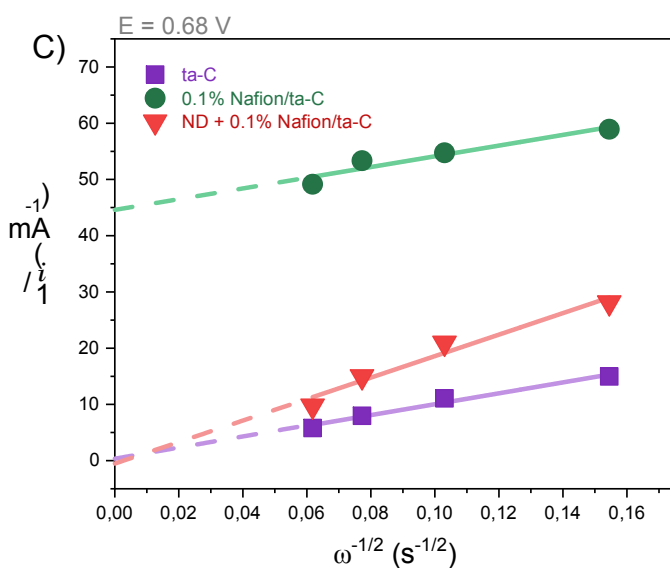


Figure 7 Electrochemical performance of A) DND + 0.1 Nafion/ta-C and B) DND + 5% Nafion/ta-C in 1 mM UA in 10 mM PBS. C) Koutecký-Levich plot at $E = 0.68$ V showing kinetic currents for plain ta-C, 0.1% Nafion/ta-C and DND + 0.1% Nafion/ta-C in 1 mM UA. Scan rate for all measurements $v = 50$ mV/s.

For 5% Nafion/ta-C cyclic voltammograms in UA are shown in Figure 7B. In PBS peak currents for Nafion characteristic reactions are enhanced as DNDs are introduced into the polymer. Interestingly, currents are further increased in presence of UA. As discussed in section 4.3, with the thickest film uric is either blocked or masked by the Nafion's own characteristic reactions. Thus, it is difficult to evaluate how the addition of DNDs alters the electrochemical detection of UA. However, results in Figure 6B demonstrate that introducing DNDs into 5% Nafion also changes the chemical properties of the polymer film. As UA enhances the redox peaks of DND + 5% Nafion film, it is clear that chemical interactions take place between the analyte and composite film.

To summarize, addition of nanodiamonds alters significantly the electrochemical performance of Nafion films. With inner sphere probe UA addition of DNDs is observed already in 0.1% Nafion film, whereas with outer sphere probes $\text{Ru}(\text{NH}_3)_6^{2+/3+}$ and $\text{IrCl}_6^{3-/4-}$ difference in Nafion performance is not seen until 5% Nafion. In all of these three cases adding carboxyl functionalized DNDs to Nafion enhanced kinetics of the electrode reactions i.e. analytes diffuse more easily through the Nafion film. When the selectivity of the electrodes is assessed, it is clear that DNDs reduces Nafion's selectivity towards anionic species. As these results only demonstrates interactions between DNDs and Nafion, we emphasize the importance of case specific characterization of the Nafion membrane selectivity against thickness when other materials, such as carbon nanotubes or enzymes, are incorporated in Nafion.

5. Conclusions

Here we highlight the importance of optimizing Nafion film thickness in selective detection of cations under physiological conditions. With extremely thin film (0.1% Nafion) anionic limiting currents are significantly decreased. However, the film does not completely block anionic species. With thicker Nafion (~3.6 μm) layers $\text{Ru}(\text{NH}_3)_6^{2+/3+}$ strongly enriches the film. However, electrochemical performance of thicker Nafion layers are heavily dependent on the width of the potential window used. Therefore, detection of cationic analytes of interest may be masked by Nafion own redox reactions.

Furthermore, we also showed that modifying the Nafion film with nanodiamonds increases analytes permeability through the membrane. Overall kinetics increased with the thickest composite film (DND + 5% Nafion) with outer sphere probes $\text{Ru}(\text{NH}_3)_6^{2+/3+}$ and $\text{IrCl}_6^{3-/4-}$. Interestingly, with the inner sphere probe UA enhanced kinetics (most likely arising from chemical interactions) were already seen with extremely thin composite film (DND + 0.1% Nafion). As diffusion of anionic species, especially UA, increases through the film, it is concluded that the addition of DNDs reduces the selectivity of Nafion membrane. This phenomena may occur other materials as well. Therefore it is an important factor that must be taken into account when numerous results from the literature related to Nafion mixtures are considered. In fact, addition of other substances to Nafion may also induce chemical effects as shown here by the interplay between DNDs and UA.

As these experiments were conducted *in vitro* with simple solutions, in the future work Nafion thickness should be optimized in more complex biological environments to address protein adsorption, for instance. Additionally when fabricating Nafion composite film, selectivity of the material need to be characterized in presence of interferents specific for the application environment.

Acknowledgements

Finnish Funding Agency for Technology and Innovation (FEDOC project, grant number 211637) is acknowledged for funding this research. M.Sc. Jarkko Etula and M.Sc. Niklas Wester are acknowledged for ta-C fabrication.

References

- [1] K.A. Mauritz, R.B. Moore, State of understanding of Nafion, *Chem. Rev.* 104 (2004) 4535–4585. doi:10.1021/cr0207123.
- [2] D. Zheng, J. Ye, L. Zhou, Y. Zhang, C. Yu, Simultaneous determination of dopamine, ascorbic acid and uric acid on ordered mesoporous carbon/Nafion composite film, *J. Electroanal. Chem.* 625 (2009) 82–87. doi:10.1016/j.jelechem.2008.10.012.
- [3] D. Kim, S. Lee, Y. Piao, Electrochemical determination of dopamine and acetaminophen

using activated graphene-Nafion modified glassy carbon electrode, *J. Electroanal. Chem.* 794 (2017) 221–228. doi:10.1016/j.jelechem.2017.04.018.

- [4] F.-F. Zhang, Q. Wan, C.-X. Li, X.-L. Wang, Z.-Q. Zhu, Y.-Z. Xian, L.-T. Jin, K. Yamamoto, Simultaneous monitoring of glucose, lactate, l-glutamate and hypoxanthine levels in rat striatum by a flow-injection enzyme electrode array system with in vivo microdialysis sampling, *J. Electroanal. Chem.* 575 (2005) 1–7. doi:10.1016/J.JELECHEM.2004.07.039.
- [5] M. Shamsipur, Z. Karimi, M. Amouzadeh Tabrizi, S. Rostamnia, Highly sensitive non-enzymatic electrochemical glucose sensor by Nafion/SBA-15-Cu (II) modified glassy carbon electrode, *J. Electroanal. Chem.* 799 (2017) 406–412. doi:10.1016/J.JELECHEM.2017.06.029.
- [6] N. Wisniewski, M. Reichert, Methods for reducing biosensor membrane biofouling, *Colloids Surfaces B Biointerfaces.* 18 (2000) 197–219. doi:10.1016/S0927-7765(99)00148-4.
- [7] M. Watanabe, H. Igarashi, K. Yosioka, An experimental prediction of the preparation condition of Nafion-coated catalyst layers for PEFCs, *Electrochim. Acta.* 40 (1995) 329–334. doi:10.1016/0013-4686(94)00271-2.
- [8] T.J. Schmidt, H.A. Gasteiger, G.D. Stäb, P.M. Urban, D.M. Kolb, R.J. Behm, Characterization of high-surface-area electrocatalysts using a rotating disk electrode configuration, *J. Electrochem. Soc.* 145 (1998) 2354–2358. doi:10.1149/1.1838642.
- [9] Z. Lin, J. Chen, G. Chen, An ECL biosensor for glucose based on carbon-nanotube/Nafion film modified glass carbon electrode, *Electrochim. Acta.* 53 (2008) 2396–2401. doi:10.1016/J.ELECTACTA.2007.09.063.
- [10] L. Qu, Y. Yin, R. Yang, G. Li, S. Yang, J. Li, Nano-sized copper oxide/multi-wall carbon nanotube/Nafion modified electrode for sensitive detection of dopamine, *J. Electroanal. Chem.* 703 (2013) 45–51. doi:10.1016/j.jelechem.2013.04.020.
- [11] E. Nagles, L. Ibarra, J.P. Llanos, J. Hurtado, O. Garcia-Beltrán, Development of a novel electrochemical sensor based on cobalt(II) complex useful in the detection of dopamine in presence of ascorbic acid and uric acid, *J. Electroanal. Chem.* 788 (2017) 38–43. doi:10.1016/j.jelechem.2017.01.057.
- [12] Z. Miao, P. Wang, A. Zhong, M. Yang, Q. Xu, S. Hao, X. Hu, Development of a glucose biosensor based on electrodeposited gold nanoparticles–polyvinylpyrrolidone–polyaniline nanocomposites, *J. Electroanal. Chem.* 756 (2015) 153–160.

doi:10.1016/J.JELECHEM.2015.08.025.

- [13] Y.-C. Luo, J.-S. Do, Urea biosensor based on PANi(urease)-Nafion®/Au composite electrode, *Biosens. Bioelectron.* 20 (2004) 15–23. doi:10.1016/J.BIOS.2003.11.028.
- [14] T. Palomäki, N. Wester, M.A. Caro, S. Sainio, V. Protopopova, J. Koskinen, T. Laurila, Electron transport determines the electrochemical properties of tetrahedral amorphous carbon (ta-C) thin films, *Electrochim. Acta.* 225 (2017) 1–10. doi:10.1016/J.ELECTACTA.2016.12.099.
- [15] S. Sainio, D. Nordlund, M.A. Caro, R. Gandhiraman, J. Koehne, N. Wester, J. Koskinen, M. Meyyappan, T. Laurila, Correlation between sp^3 -to- sp^2 Ratio and Surface Oxygen Functionalities in Tetrahedral Amorphous Carbon (ta-C) Thin Film Electrodes and Implications of Their Electrochemical Properties, *J. Phys. Chem. C.* 120 (2016) 8298–8304. doi:10.1021/acs.jpcc.6b02342.
- [16] M.A. Caro, A. Aarva, V.L. Deringer, G. Csányi, T. Laurila, Reactivity of Amorphous Carbon Surfaces: Rationalizing the Role of Structural Motifs in Functionalization Using Machine Learning, *Chem. Mater.* 30 (2018) 7446–7455. doi:10.1021/acs.chemmater.8b03353.
- [17] V.L. Deringer, M.A. Caro, R. Jana, A. Aarva, S.R. Elliott, T. Laurila, G. Csányi, L. Pastewka, Computational Surface Chemistry of Tetrahedral Amorphous Carbon by Combining Machine Learning and Density Functional Theory, *Chem. Mater.* 30 (2018) 7438–7445. doi:10.1021/acs.chemmater.8b02410.
- [18] M.A. Caro, V.L. Deringer, J. Koskinen, T. Laurila, G. Csányi, Growth Mechanism and Origin of High sp^3 Content in Tetrahedral Amorphous Carbon, *Phys. Rev. Lett.* 120 (2018) 166101. doi:10.1103/PhysRevLett.120.166101.
- [19] J. Robertson, Diamond-like amorphous carbon, *Mater. Sci. Eng. R Reports.* 37 (2002) 129–281. doi:10.1016/S0927-796X(02)00005-0.
- [20] E. Kaivosoja, P. Suvanto, G. Barreto, S. Aura, A. Soininen, S. Franssila, Y.T. Konttinen, Cell adhesion and osteogenic differentiation on three-dimensional pillar surfaces, *J. Biomed. Mater. Res. - Part A.* 101 A (2013) 842–852. doi:10.1002/jbm.a.34378.
- [21] T. Laurila, V. Protopopova, S. Rhode, S. Sainio, T. Palomäki, M. Moram, J.M. Feliu, J. Koskinen, New electrochemically improved tetrahedral amorphous carbon films for biological applications, *Diam. Relat. Mater.* 49 (2014) 62–71. doi:10.1016/j.diamond.2014.08.007.
- [22] N. Wester, J. Etula, T. Lilius, S. Sainio, T. Laurila, J. Koskinen, Selective detection of

morphine in the presence of paracetamol with anodically pretreated dual layer Ti/tetrahedral amorphous carbon electrodes, *Electrochem. Commun.* 86 (2018) 166–170.

doi:10.1016/J.ELECOM.2017.12.014.

- [23] E. Mynttinen, N. Wester, T. Lilius, E. Kalso, J. Koskinen, T. Laurila, Simultaneous electrochemical detection of tramadol and O-desmethyltramadol with Nafion-coated tetrahedral amorphous carbon electrode, *Electrochim. Acta.* 295 (2019) 347–353. doi:10.1016/J.ELECTACTA.2018.10.148.
- [24] V. Yu. Dolmatov, Up-to-date commercial production technology for detonation nanodiamonds and their main applications. Report 1, (2006) 12. <http://udiamonds.ru/production-technology/> (accessed August 3, 2016).
- [25] S. Osswald, G. Yushin, V. Mochalin, S. O. Kucheyev, Y. Gogotsi, Control of sp²/sp³ Carbon Ratio and Surface Chemistry of Nanodiamond Powders by Selective Oxidation in Air, *J. Am. Chem. Soc.* 128 (2006) 11635-11642. doi: 10.1021/ja063303n.
- [26] I.I. Kulakova, Surface chemistry of nanodiamonds, *Phys. Solid State.* 46 (2004) 636–643. doi:10.1134/1.1711440.
- [27] K.B. Holt, Undoped diamond nanoparticles: origins of surface redox chemistry, *Phys. Chem. Chem. Phys.* 12 (2010) 2048. doi:10.1039/b920075d.
- [28] K.B. Holt, C. Ziegler, D.J. Caruana, J. Zang, E.J. Millán-Barrios, J. Hu, J.S. Foord, Redox properties of undoped 5 nm diamond nanoparticles, *Phys. Chem. Chem. Phys.* 10 (2008) 303–310. doi:10.1039/B711049A.
- [29] K.B. Holt, C. Ziegler, J. Zang, J. Hu, J.S. Foord, Scanning Electrochemical Microscopy Studies of Redox Processes at Undoped Nanodiamond Surfaces, *J. Phys. Chem. C.* 113 (2009) 2761–2770. doi:10.1021/jp8038384.
- [30] T.S. Varley, M. Hirani, G. Harrison, K.B. Holt, Nanodiamond surface redox chemistry: influence of physicochemical properties on catalytic processes, *Faraday Discuss.* 172 (2014) 349–364. doi:10.1039/C4FD00041B.
- [31] K.B. Holt, D.J. Caruana, E.J. Millán-Barrios, Electrochemistry of Undoped Diamond Nanoparticles: Accessing Surface Redox States, *J. Am. Chem. Soc.* 131 (2009) 11272-11273. doi: 10.1021/ja902216n.
- [32] L.H. Chen, J.B. Zang, Y.H. Wang, L.Y. Bian, Electrochemical oxidation of nitrite on

nanodiamond powder electrode, *Electrochim. Acta.* 53 (2008) 3442–3445.

doi:10.1016/j.electacta.2007.12.023.

- [33] J. Zang, Y. Wang, L. Bian, J. Zhang, F. Meng, Y. Zhao, S. Ren, X. Qu, Surface modification and electrochemical behaviour of undoped nanodiamonds, *Electrochim. Acta.* 72 (2012) 68–73. doi:10.1016/j.electacta.2012.03.169.
- [34] E. Peltola, N. Wester, K.B. Holt, L.-S. Johansson, J. Koskinen, V. Myllymäki, T. Laurila, Nanodiamonds on tetrahedral amorphous carbon significantly enhance dopamine detection and cell viability, *Biosens. Bioelectron.* 88 (2017) 273–282. doi:10.1016/J.BIOS.2016.08.055.
- [35] A.J. Bard, L.R. Faulkner, *Electrochemical methods: Fundamentals and applications*, 2nd ed., New York, 2001.
- [36] D.A. Gough, J.K. Leypoldt, Membrane-Covered, Rotated Disc Electrode, *Anal. Chem.* 51 (1979) 439–444. doi:10.1021/ac50039a028.
- [37] D.A. Gough, J.K. Leypoldt, Rotated, Membrane-Covered Oxygen Electrode, *Anal. Chem.* 52 (1980) 1126–1130. doi:10.1021/ac50057a030.
- [38] A. Krüger, F. Kataoka, M. Ozawa, T. Fujino, Y. Suzuki, A.E. Aleksenskii, A.Y. Vul', E. Ōsawa, Unusually tight aggregation in detonation nanodiamond: Identification and disintegration, *Carbon N. Y.* 43 (2005) 1722–1730. doi:10.1016/J.CARBON.2005.02.020.
- [39] A. Kumar, P. Ann Lin, A. Xue, B. Hao, Y. Khin Yap, R.M. Sankaran, Formation of nanodiamonds at near-ambient conditions via microplasma dissociation of ethanol vapour, *Nat. Commun.* 4 (2013) 1–8. doi:10.1038/ncomms3618.
- [40] H. Hirai, K.I. Kondo, Modified phases of diamond formed under shock compression and rapid quenching, *Science (80-.)*. 253 (1991) 772–774. doi:10.1126/science.253.5021.772.
- [41] R.H. Wopschall, I. Shain, Effects of Adsorption of Electroactive Species in Stationary Electrode Polarography, *Anal. Chem.* 39 (1967) 1514–1527. doi:10.1021/ac50156a018.
- [42] P.-Y. Chen, R. Vittal, P.-C. Nien, K.-C. Ho, Enhancing dopamine detection using a glassy carbon electrode modified with MWCNTs, quercetin, and Nafion[®], *Biosens. Bioelectron.* 24 (2009) 3504–3509. doi:10.1016/j.bios.2009.05.003.
- [43] L. Yang, X. Ren, F. Tang, L. Zhang, A practical glucose biosensor based on Fe₃O₄ nanoparticles and chitosan/nafion composite film, *Biosens. Bioelectron.* 25 (2009) 889–895. doi:10.1016/J.BIOS.2009.09.002.

- [44] M. Jamal, J. Xu, K.M. Razeed, Disposable biosensor based on immobilisation of glutamate oxidase on Pt nanoparticles modified Au nanowire array electrode, *Biosens. Bioelectron.* 26 (2010) 1420–1424. doi:10.1016/J.BIOS.2010.07.071.
- [45] J.J. Burmeister, G.A. Gerhardt, Self-referencing ceramic-based multisite microelectrodes for the detection and elimination of interferences from the measurement of L-glutamate and other analytes, *Anal. Chem.* 73 (2001) 1037–1042.